

# Neural sources involved in auditory target detection and novelty processing: An event-related fMRI study

KENT A. KIEHL,<sup>a</sup> KRISTIN R. LAURENS,<sup>a</sup> TIMOTHY L. DUTY,<sup>b</sup> BRUCE B. FORSTER,<sup>c</sup>  
AND PETER F. LIDDLE<sup>a</sup>

<sup>a</sup>Departments of Psychology and Psychiatry, University of British Columbia, Vancouver, B.C., Canada

<sup>b</sup>Department of Physics, University of British Columbia, Vancouver, B.C., Canada

<sup>c</sup>Department of Radiology, University of British Columbia, Vancouver, B.C., Canada

## Abstract

We used event-related functional magnetic resonance imaging (erfMRI) techniques to examine the cerebral sites involved with target detection and novelty processing of auditory stimuli. Consistent with the results from a recent erfMRI study in the visual modality, target processing was associated with activation bilaterally in the anterior superior temporal gyrus, inferior and middle frontal gyrus, inferior and superior parietal lobules, anterior and posterior cingulate, thalamus, caudate, and the amygdala/hippocampal complex. Analyses of the novel stimuli revealed activation bilaterally in the inferior frontal gyrus, insula, inferior parietal lobule, and in the inferior, middle, and superior temporal gyri. These data suggest that the scalp recorded event-related potentials (e.g., N2 and P3) elicited during similar tasks reflect an ensemble of neural generators located in spatially remote cortical areas.

**Descriptors:** Functional magnetic resonance imaging, Target detection, Novelty processing, Auditory

More than three decades ago, Sutton, Tueting, Zubin, and John (1967) reported that low-probability, unexpected auditory stimuli elicited a large positive wave at approximately 300 ms (P3) in the averaged evoked brain potential. This discovery that cognitive activity could modulate brain potentials revolutionized psychophysiological research. It is now known that the amplitude and latency of the P3 are modulated by a variety of experimental manipulations, including stimulus probability, task difficulty, and task demands (Donchin & Coles, 1988). These observations have led to the suggestion that the P3 reflects processes related to attention, decision making, and memory updating. The P3 also has been shown to be abnormal in a variety of clinical conditions, including schizophrenia, depression, and psychopathy (Ford et al., 1994; Kiehl, Hare, McDonald, & Liddle, 1999; McCarley, Faux, Shenton, Nestor, & Adams, 1991). The utility of the P3 for examining cognitive processes and characterizing clinical conditions has made it a valuable tool in the psychophysiological's repertoire. In addition

to the canonical P3, or P3b, several studies have shown that low-probability, task-irrelevant novel stimuli elicit a P3 with an earlier latency and more anterior scalp distribution (Knight, 1984). The novelty P3, or P3a, is thought to reflect processes related to the orienting response.

Although the time course and scalp topography of the P3 is well characterized, considerable controversy persists regarding the neural generators of the both the P3a and P3b. Converging evidence from magnetoencephalography (MEG), positron emission tomography (PET), intracranial recordings, and data from patients with brain lesions suggest that the thalamus, inferior parietal lobe, temporal lobe, dorsolateral prefrontal cortex, cingulate cortex, amygdala, hippocampal formation, and orbital frontal cortex may be involved in generating the scalp recorded P3 (Halgren, Marinkovic, & Chauvel, 1998). More specifically, using evidence from intracranial studies, Halgren and colleagues argued that target processing is associated with neural activity in the hippocampal formation, superior temporal gyrus, lateral orbital frontal gyrus, and supramarginal gyrus. Halgren et al. also observed that processing rare stimuli is associated with time-locked neural activity in the cingulate, dorsolateral prefrontal cortex, and inferior parietal lobule. These latter areas are believed to be involved in the orienting response to the rare stimuli (see Halgren et al., 1998, for a review).

Recent developments in functional magnetic resonance (fMRI) imaging have shown that it is possible to measure the hemodynamic response from individually presented events. Event-related fMRI (erfMRI), as it has been coined, has opened up a new genre of experimental protocols for hemodynamic imaging (Josephs, Turner, & Friston, 1997; Rosen, Buckner, & Dale, 1998). For example, several groups of investigators have performed er-

---

This research was supported in part by grants from the Norma Calder Society, Medical Research Council (MRC) of Canada, the British Columbia Health Services, the British Columbia Medical Services Foundation and funds from the Schizophrenia Division, Department of Psychiatry, University of British Columbia. K.A.K. was supported by the Michael Smith Graduate Scholarship, Medical Research Council of Canada.

We thank Drs. Alex MacKay and Ken Whittall and MR technicians Trudy Shaw, Karen Smith, and Sylvia Renneberg for their assistance. We also thank several anonymous reviewers for their constructive comments on an earlier draft of this manuscript.

Address reprint requests to: Kent A. Kiehl, 2255 Wesbrook Mall, Department of Psychiatry, University of British Columbia, Vancouver, B.C., V6T 2A1, Canada. E-mail: kiehl@cs.ubc.ca.

fMRI studies of cerebral activity associated with processing low probability stimuli. McCarthy, Luby, Gore, and Goldman-Rakic (1997) found that low probability visual stimuli elicited activation in the middle frontal gyrus, inferior parietal lobe, and in the posterior cingulate. Menon, Ford, Lim, Glover, and Pfefferbaum (1997) found that target stimuli in the auditory modality generated activity in the inferior parietal lobe, thalamus, and anterior cingulate. Opitz, Mecklinger, Von Cramon, and Kruggel (1999), using a blocked fMRI design, found that target and deviant stimuli elicited activation in the transverse/superior temporal gyrus and neostriatum. Using an MR pulse sequence that allowed imaging of the entire brain, we (Kiehl, Laurens, Duty, Forster, & Liddle, 1999, submitted) found that low-probability, task-relevant target visual stimuli elicit activation in bilateral anterior superior temporal gyrus, amygdala, thalamus, inferior and superior parietal lobules, inferior frontal gyrus, anterior and posterior cingulate, and lateral frontal cortex. We also observed that low-probability, task-irrelevant novel stimuli generated activation in the cingulate, dorsolateral prefrontal cortex, and inferior and superior parietal lobule.

To the extent that the cerebral sites activated during these fMRI paradigms reflect the generators of the scalp-recorded P3 event-related potential (ERP), the observed pattern of hemodynamics suggested that the P3 is generated from a concert of spatially remote processing units. It should be noted, however, that it is not possible to precisely determine whether the observed hemodynamics reflect the generators of the P3 and/or other electrical components such as the N2, a negative potential observed approximately 200 ms after stimulus presentation.

Many investigators have shown that the scalp-recorded P3 can be elicited reliably in the visual, auditory, and somatosensory modalities, suggesting that this P3 is independent of stimulus modality. The purpose of the present study was to elucidate the cerebral sites activated during auditory target detection and novelty processing and to compare these sources with our previous findings in the visual modality. We used an experimental methodology identical to that in our previous study of visual target detection and novelty processing (Kiehl et al., 1999, submitted), in which we presented stimuli every 2 s, with a random 6–10-s interval between target and novel stimuli. Three to five nontarget stimuli occurred between consecutive target and novel stimuli.

On the basis of our findings from the visual modality study, we predicted that for target stimuli there would be activation bilaterally in the anterior superior temporal gyrus, inferior and superior parietal lobule, inferior frontal gyrus, cingulate, thalamus, amygdala, and lateral frontal cortex. We also predicted that novelty processing would be associated with activation in dorsolateral prefrontal cortex, cingulate, temporal lobes, and parietal lobes.

In addition to examining the activations for the target and novel stimuli (relative to the baseline of nontarget processing), we also directly contrasted target stimuli versus novel stimuli, and novel stimuli versus target stimuli, respectively. These latter contrasts were included to examine the areas in which significant differences in the hemodynamic response occurred between target and novel stimuli.

## Methods

### Participants

Ten healthy right-handed volunteers (5 men and 5 women, mean age 26.3 years,  $SD = 7.2$ ) participated in the study. Participants provided written informed consent and were screened for MRI compatibility before entry into the scanning room. All experimental procedures met with University and Hospital ethical approval.

### Procedure

Two runs of 244 stimuli were presented to the participant by a computer-controlled auditory sound system that delivered the auditory stimuli with insert earphones embedded within 30-dB sound-attenuating MR compatible headphones. The nontarget stimulus was a 1000-Hz tone, the target stimulus was a 1500-Hz tone, and the novel stimuli consisted of nonrepeating random digital noises (e.g., tone sweeps, whistles). All stimuli were presented at approximately 80 dB. All participants reported that they could hear the stimuli and discriminate them from the background scanner noise (see the results of the behavioral data).

The target and novel stimuli each occurred with a probability of .125; the nontarget stimuli occurred with a probability of .75. The stimulus duration was 200 ms with a 2,000-ms interstimulus interval (ISI). The rate of stimulus presentation is similar to that typically used in analogous ERP studies (Alexander et al., 1996). Target and novel stimuli were always preceded by at least three nontarget stimuli (range three to five). The intervals between stimuli of interest (i.e., target and novel stimuli) were allocated in a pseudorandom manner in the range of 6–10 s so as to ensure that these stimuli had equal probability of occurring at 0, 1, and 2 s after the beginning of a 3-s image acquisition period. As a result, the hemodynamic response to each type of stimulus of interest was sampled uniformly at 1-s intervals. A custom visual and auditory presentation package was used to tightly couple the presentation of the stimuli with the acquisition of the MR scanner.

Participants were instructed to respond as quickly and as accurately as possible with their right index finger every time the target tone occurred and not to respond to the nontarget tones or the novel stimuli. A commercially available MRI compatible fiberoptic response device (Lightwave Medical, Vancouver, B.C.) was used to acquire behavioral responses. Reaction times were computed on trials for which the participant responded correctly within 1,200 ms poststimulus. Omission errors included any missed target tones or any response with a latency of longer than 1,200 ms after the onset of the target stimulus. Errors of commission were defined as responses following the nontarget or novel stimuli within 1,200 ms of stimulus onset. Before entry into the scanning room, each participant performed a practice block of 10 trials to ensure understanding of the instructions.

*Imaging parameters.* Imaging was implemented on a standard clinical GE 1.5 T system fitted with a Horizon Echo-speed upgrade. The participant's head was firmly secured using a custom head holder. Conventional spin-echo  $T_1$ -weighted sagittal localizers were acquired to view the positioning of the participant's head in the scanner and to graphically prescribe the functional image volumes. Functional image volumes were collected with a gradient-echo sequence (TR/TE 3000/40 ms, flip angle 90°, FOV 24 × 24 cm, 64 × 64 matrix, 62.5 kHz bandwidth, 3.75 × 3.75 mm in plane resolution, 5 mm slice thickness, 29 slices) effectively covering the entire brain (145 mm). This sequence is sensitive to the blood oxygen level dependent contrast (see review by D'Esposito, Zarahn, & Aguirre, 1999). The two stimulus runs consisted of 167 time points, prefaced by a 12-s rest session that was collected to allow for  $T_1$  effects to stabilize. These initial images were not included in any subsequent analyses.

*Image processing.* Functional images were reconstructed offline and the two runs were separately realigned using the procedure by Friston, Williams, Howard, Frackowiak, and Turner (1996) as implemented in Statistical Parametric Mapping (SPM97,

Wellcome Department of Cognitive Neurology; Friston et al., 1995a). Translation and rotation corrections did not exceed 1.5 mm and 1.5 degrees, respectively, for any of the participants. A mean functional image volume was constructed for each participant for each run from the realigned image volumes. This mean image volume was then used to determine parameters for spatial normalization into the modified Talairach space used in SPM97 using both affine and nonlinear components (Friston et al., 1995b). In this space, coordinates are expressed relative to a rectangular coordinate frame with the origin at the midpoint of the anterior commissure and the  $y$ -axis passing through the posterior and anterior commissures. The normalization parameters determined for the mean functional volume were then applied to the corresponding functional image volumes for each participant. The normalized functional images were then smoothed with an 8-mm full width at half-maximum Gaussian filter to yield a smoothness in the final analyses of 10.9, 11.0, 10.6 mm in the  $x$ ,  $y$ , and  $z$  dimensions, respectively.

Event-related responses to the target and novel stimuli were modeled using a synthetic hemodynamic response function composed of two gamma functions (see Josephs et al., 1997, for mathematical model; and Friston et al., 1998, for illustration). The first gamma function modeled the hemodynamic response using a peak latency of 6 s. A term proportional to the derivative of this gamma function was included to allow for small variations in peak latency. The second gamma function and associated derivative was used to model the small “overshoot” of the hemodynamic response on recovery. The modeled composite hemodynamic response for each run was derived by constructing a sequence of appropriately located synthetic responses for target stimuli and for novel stimuli. Because nontarget stimuli were presented at the rate of once every 2 s with the object of maintaining a sustained hemodynamic response that did not vary substantially throughout the task, the response to the nontarget stimuli was treated as the baseline (for the first two comparisons, see below) and therefore not included in the model. Because multiple voxels were examined, a correction for multiple comparisons based on the theory of Gaussian fields was used (Worsley, 1994; Worsley & Friston, 1995). Reported statistical levels are significant at the voxel level (Worsley & Friston, 1995) and were all greater than  $p < .05$  corrected for multiple comparisons unless otherwise noted. A high-pass filter (cut-off period 89 s) was incorporated into the model and remove noise associated with low frequency confounds (e.g., respiratory artifact; see Holmes, Josephs, Buchel, & Friston, in press). We also applied a low-pass filter at the Nyquist frequency (period of 6 seconds) to remove noise associated with alternations of the applied radio frequency field. All images were normalized to a mean of 100 (arbitrary units) for each run to compensate for any intensity variations across runs. In addition to this intensity normalization, we also performed an additional analysis in which we used a proportional scaling technique to compensate for global signal variation (Fox, Mintun, Reiman, & Raichle, 1984; Friston et al., 1990). This latter analysis was performed to address the issue that excessive Type II errors are possible when comparing conditions in which one condition produces much more activation than another. In our study, the target detection condition produced about 30% more activated voxels than did the novelty processing condition, which may lead to a conservative bias in the comparison of the novel stimuli with the target stimuli (see Andersson, 1997). For these reasons we report the areas of activation for comparisons involving novel stimuli using this latter analysis. We note however, that in all cases, the areas of activation reported were significant in

both analyses, regardless of global normalization, at a  $z$  score value greater than 1.97, corresponding to  $p < .05$ , uncorrected significance level.

The advantage of modeling the hemodynamic response in terms of basis functions, in this case, gamma functions and their derivatives, is fourfold. First, it has been shown that these gamma functions provide both reasonable and comprehensive models of the hemodynamic response (Boynton, Engel, Glover, & Heeger, 1996; Friston, Jezzard, & Turner, 1994). Second, by fitting the hemodynamic response for each voxel, we were able to effectively model variations in the hemodynamic response in both amplitude and latency between different brain regions and between different events. Third, the creation of the parameter estimates in terms of peristimulus time allows us to achieve an effective temporal resolution less than the total acquisition time (Josephs et al., 1997). This temporal resolution cannot be achieved using standard averaging techniques (akin to ERP studies). Lastly, formulating the model in this way allows us to use standard procedures developed for analyzing serially correlated fMRI time series that use the general linear model and a sound theoretical correction for the number of comparisons examined (Friston et al., 1995a; Worsley & Friston, 1995). We note, however, that the technique we used for modeling event-related responses is controversial. In particular, the technique we used assumed that the events must occur repeatedly and must elicit stereotyped and reproducible responses. We have also assumed linear hemodynamic response functions. Recent fMRI studies suggest that there may be nonlinear components of

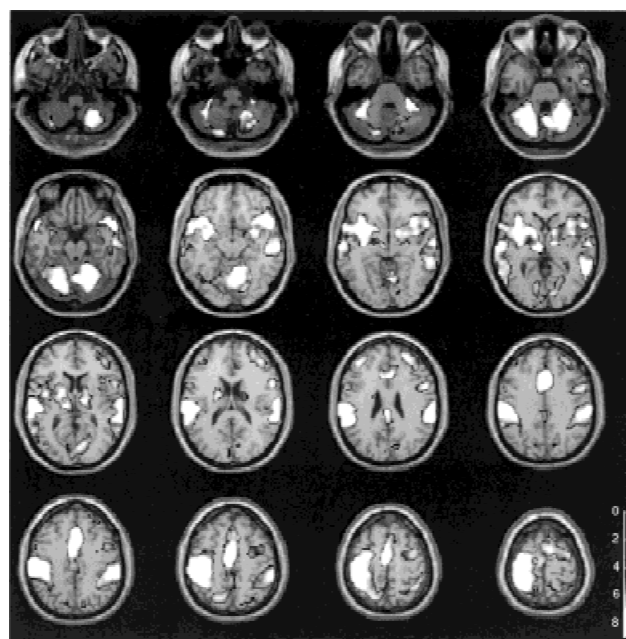


**Figure 1.** Illustration of the areas of activation for the comparison of the target stimuli versus the nontarget baseline condition. Data are presented in the modified Talairach space used in Statistical Parametric Mapping (SPM97, Wellcome Department of Cognitive Neurology; Friston et al., 1995a) and is rendered onto a standard reference brain (the left hemisphere is on the left). Starting at the top left corner and progressing from left to right, the  $z$  levels in standard space are, first row:  $-52$ ,  $-44$ ,  $-36$ ,  $-28$  mm; second row:  $-20$ ,  $-12$ ,  $-4$ ,  $4$  mm; third row:  $12$ ,  $20$ ,  $28$ ,  $36$  mm; last row:  $44$ ,  $52$ ,  $60$ , and  $68$  mm, respectively.

the hemodynamic response (Dale & Buckner, 1997; Friston, Zarahn, Josephs, Henson, & Dale, 1999). These nonlinear components appear to be most prevalent for studies using short ISIs (e.g., less than 1 s). However, in the present experiment, events of interest (e.g., targets and novel stimuli) were spaced 6–10 s apart, thus decreasing the likelihood that nonlinearities may have affected the data. Thus, the validity of our conclusions depends on the correctness of the SPM model. More details on these issues can be found in Buckner (1998), Friston et al. (1999), and Rosen et al. (1998).

To summarize, the multisubject ( $n = 10$ ) statistical analysis was constructed using a design matrix that included separate gamma functions and their respective temporal derivatives for both the target and novel stimuli, a block effect (i.e., intensity normalization), low-pass filter, and a notch filter. The resulting SPM (F)

contained voxels in which the model effectively characterized the observed data. Four contrasts were then used to create SPM(t)s for our comparisons of interest. The SPM(t)s were then transformed into SPM(Z)s. The four comparisons were: (1) activations for the target stimuli relative to the nontarget baseline condition; (2) activations for the novel stimuli relative to the nontarget baseline; (3) direct comparison of the target stimuli versus novel stimuli; and (4) a direct comparison of the novel stimuli versus target stimuli.

## Results

### Behavioral Data

The mean reaction time and percentage of correct hits was 412 ms ( $SD = 56.23$ ) and 98.4% ( $SD 1.47$ ), respectively. False alarms to

**Table 1.** Summary of the Significant Areas of Activation for the Comparison of the Target Stimuli Versus the Nontarget Baseline Condition

Region	Talairach coordinates			z score
	x	y	z	
Frontal lobes				
1. L superior/middle frontal gyrus	-30	50	30	6.62
2. R superior/middle frontal gyrus	26	52	30	7.41
3. L inferior frontal gyrus	-60	8	25	7.04
4. R inferior frontal gyrus	56	11	25	7.55
5. Medial frontal gyrus	0	-8	55	8.41
6. Anterior cingulate gyrus	0	16	40	8.26
7. L insula	-38	19	-10	7.65
8. R insula	44	24	-10	7.39
9. L precentral gyrus	-38	-26	65	8.96
10. R precentral gyrus	38	-4	60	7.08
Parietal lobes				
11. L postcentral gyrus	-56	-22	20	8.59
12. L postcentral gyrus	-26	-44	65	8.03
13. R postcentral gyrus	68	-19	20	8.25
14. L superior parietal lobule	-38	-48	60	7.94
15. R superior parietal lobule	24	-60	55	5.78
16. L inferior parietal/supramarginal gyrus	-56	-41	30	8.30
17. R inferior parietal/supramarginal gyrus	64	-34	25	8.05
18. Posterior cingulate gyrus	0	-30	30	7.43
19. Precuneus	0	-45	55	6.60
Temporal lobes				
20. L superior temporal gyrus	-56	11	-15	8.12
21. R superior temporal gyrus	52	19	-15	8.29
22. L middle temporal gyrus	-60	-56	5	7.18
23. R middle temporal gyrus	52	-22	-10	7.76
24. L inferior temporal gyrus	-54	-18	-15	5.55
25. R inferior temporal gyrus	60	-64	5	6.91
26. L parahippocampal gyrus/amygdala	-18	-4	-20	6.30
27. R parahippocampal gyrus/amygdala	20	-2	-20	5.41
Occipital lobes				
28. L lingual gyrus/cuneus	-11	-71	5	6.98
29. R lingual gyrus/cuneus	19	-71	10	7.51
Deep gray				
30. L thalamus/caudate	-8	-19	5	7.98
31. R thalamus/caudate	11	-15	5	7.60
32. L putamen/globus pallidus	-38	0	-5	7.85
33. R putamen/globus pallidus	26	0	0	7.17
Cerebellum				
34. L cerebellum	-22	-64	-25	8.04
35. R cerebellum	19	-52	-30	8.59

Note: L = left; R = right.

Probability levels associated with the z scores are: 7.02,  $p \leq .0000001$ ; 6.67,  $p \leq .000001$ ; 6.30,  $p \leq .00001$ ; 5.90,  $p \leq .0001$ ; 5.46,  $p \leq .001$ ; 4.94,  $p \leq .01$ ; and 4.62,  $p \leq .05$ . These probability levels are corrected for multiple comparisons (Worsley & Friston, 1995).

novel and nontarget stimuli were relatively rare (novel,  $M = 1.2$ ,  $SD = .8$ ; nontargets,  $M = .6$ ,  $SD = .55$ ).

**Imaging Data**

Consistent with the results from the visual oddball task, analyses of the auditory target stimuli revealed activation bilaterally in the anterior superior temporal gyrus, inferior frontal gyrus, inferior and superior parietal lobules, anterior and posterior cingulate, superior/middle frontal gyrus, thalamus, amygdala, caudate, and putamen (Table 1, Figure 1). Analyses of the target stimuli also revealed activation in the left precentral and postcentral gyrus, medial frontal gyrus, and right cerebellum consistent with the fact that the target processing required a button press using the right index finger. All areas of activation for this comparison are reported in Table 1.

Analyses of the hemodynamic response for the novel stimuli revealed activation bilaterally in the inferior, middle, and superior temporal gyrus (see Table 2, Figure 2). Consistent with the hemodynamic response to visual novel stimuli, activation was found for the novel auditory stimuli bilaterally in the inferior, middle, and medial frontal gyrus, and inferior parietal lobule and insula. Other areas of activation are listed in Table 2.

The results of the direct comparison of the target stimuli versus the novel stimuli largely paralleled the comparison of the target stimuli versus the nontarget baseline condition. In both compari-

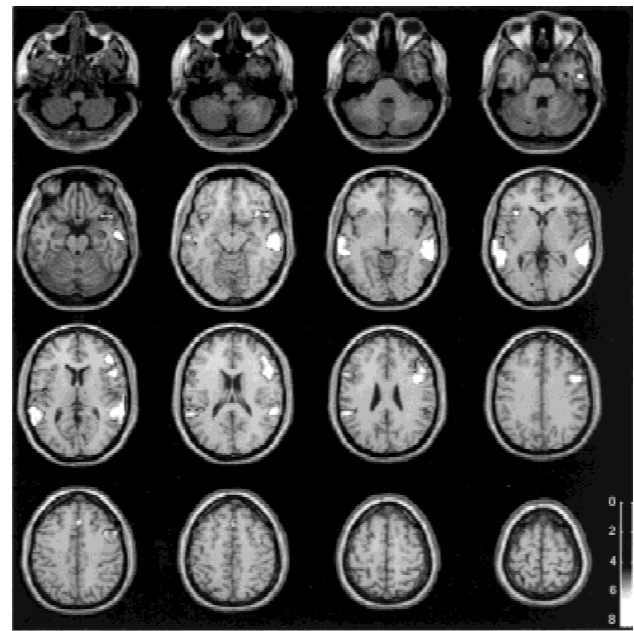


**Figure 2.** Illustration of the areas of activation for the comparison of the novel stimuli versus the nontarget baseline condition. The planes depicted are identical to those in Figure 1.

**Table 2.** Summary of the Significant Areas of Activation for the Comparison of the Novel Stimuli Versus the Nontarget Baseline Condition

Region	Talairach coordinates			z score
	x	y	z	
Frontal lobes				
1. L middle/inferior frontal gyrus	-56	15	25	6.87
2. R middle/inferior frontal gyrus	52	15	25	7.38
3. L inferior frontal gyrus/insula	-38	16	-10	5.98
4. R inferior frontal gyrus/insula	38	22	-10	6.99
5. Medial frontal gyrus	0	24	50	6.43
6. L anterior cingulate gyrus	-2	10	35	4.74
7. L insula	-40	-4	5	5.38
8. R precentral gyrus	41	8	30	7.58
Parietal lobes				
9. L postcentral gyrus	-60	-19	20	5.91
10. R postcentral gyrus	66	-18	20	6.11
11. L inferior parietal lobule	-54	-42	35	7.05
12. R inferior parietal lobule	60	-38	50	4.93
Temporal lobes				
13. L superior temporal gyrus	-62	-34	10	7.94
14. R superior temporal gyrus	49	19	-15	7.08
15. R superior temporal gyrus	58	-40	25	6.75
16. L middle temporal gyrus	-56	8	-20	6.47
17. L middle/inferior temporal gyrus	-56	-19	-5	7.21
18. R middle/inferior temporal gyrus	64	-19	-10	8.24
Occipital lobes				
19. L cuneus	-10	-80	10	4.95
20. R cuneus	12	-78	15	5.45
Deep gray				
21. L thalamus	-12	2	10	4.93
22. R thalamus	16	-12	10	4.98
Cerebellum				
23. L cerebellum	-15	-79	-35	5.44
24. R cerebellum	19	-79	-35	5.05

Note: L = left; R = right

Probability levels associated with the z scores are the same as those listed in the caption to Table 1.

sons, activation was notably greater for target processing bilaterally in the superior/middle frontal gyrus, supramarginal gyrus, inferior and superior parietal lobule, anterior superior temporal gyrus, in the anterior and posterior cingulate, insula, amygdala, and parahippocampal gyrus. Other areas in which the two conditions differed are summarized in Table 3 and illustrated in Figure 3.

Analyses of the novel versus the target stimuli comparison revealed a number of differences between the two conditions, including bilateral inferior and middle frontal gyrus, anterior and posterior cingulate, middle temporal gyrus, and inferior parietal lobule. These data are presented in Table 4 and illustrated in Figure 4.

It is important to note that there are three possible ways in which differences would be revealed in the comparison of the target stimuli with novel stimuli and for the comparison of the novel stimuli with target stimuli. First, activation for one event may be significantly greater than the activation for another event;

second, one event may show activation and the other event may show deactivation; and third, one event may show deactivation but the other event may show significantly greater deactivation. We inspected the hemodynamic response to both events in each of the significant areas activated by these contrasts to isolate which of the above differences occurred. In all cases, the observed differences between conditions were due to greater activation for one condition and little or no activation for the other condition. There were no reliable deactivations observed in the present study. Illustration of the individual hemodynamic responses for target stimuli are presented in Figure 5.

## Discussion

This study was designed to elucidate the cerebral sites involved with auditory target detection and novelty processing. In general,

**Table 3.** Summary of the Significant Areas of Activation for the Comparison of the Target Versus Novel Stimuli

Region	Talairach coordinates			z score
	x	y	z	
Frontal lobes				
1. R superior frontal gyrus	28	54	0	5.61
2. R superior/middle frontal gyrus	26	52	30	6.90
3. L middle frontal gyrus	-41	41	30	6.99
4. R middle frontal gyrus	22	0	70	6.68
5. R middle frontal gyrus	26	-4	50	4.99
6. L inferior frontal gyrus	-60	4	25	5.58
7. Medial frontal gyrus	0	-4	55	8.24
8. Anterior cingulate gyrus	0	11	45	7.86
9. R anterior cingulate gyrus	8	26	25	4.98
10. L insula	-48	4	-5	6.72
11. R insula	49	4	-5	6.88
12. L precentral gyrus	-36	-16	60	8.11
Parietal lobes				
13. L postcentral gyrus	-34	-30	70	8.90
14. R postcentral gyrus	60	-26	45	7.04
15. L superior/inferior parietal lobule	-26	-45	70	8.38
16. R superior/inferior parietal lobule	20	-50	70	6.40
17. L inferior parietal/supramarginal gyrus	-52	-41	35	6.75
18. R inferior parietal/supramarginal gyrus	49	-26	45	7.36
19. L precuneus	-15	-68	60	7.63
20. R precuneus	11	-52	70	7.70
21. Posterior cingulate gyrus	0	-34	35	5.24
Temporal lobes				
22. L superior temporal gyrus	-56	8	-10	7.46
23. R superior temporal gyrus	56	19	-20	7.22
24. R superior temporal gyrus	56	-11	5	5.65
25. L parahippocampal gyrus/amygdala	-24	-4	-15	5.74
26. R parahippocampal gyrus/amygdala	18	0	-15	4.94
27. L transverse temporal gyrus	-56	-19	15	7.96
Occipital lobes				
28. L middle occipital gyrus	-54	-68	10	5.73
29. Cuneus	0	-94	20	6.85
Deep gray				
30. L putamen	-34	0	-5	7.50
31. R putamen/globus pallidus	30	0	-10	6.28
32. L thalamus/caudate	-8	-19	5	7.11
33. R thalamus/caudate	15	0	15	6.20
Cerebellum				
34. L cerebellum	-38	-56	-25	7.32
35. R cerebellum	19	-52	-20	8.54

Note: L = left; R = right.

Probability levels associated with the z scores are the same as those listed in the caption to Table 1.

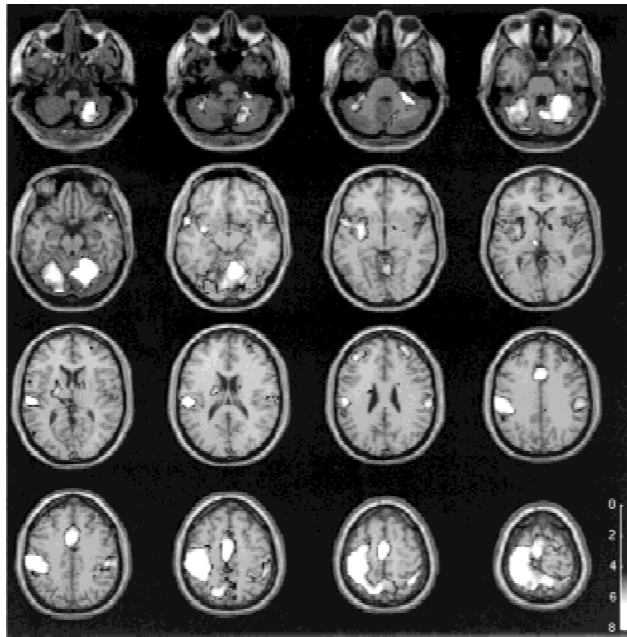


**Figure 3.** Illustration of the areas of activation for the comparison of the target stimuli versus the novel stimuli. The planes depicted are identical to those in Figure 1.

the results are consistent with recent erfMRI data on target detection and novelty processing in the visual modality from our laboratory (Kiehl et al., 1999, submitted) and others (McCarthy et al., 1997). In both modalities, target processing activated bilateral inferior frontal gyrus, anterior superior temporal gyrus, inferior and superior parietal lobules, anterior and posterior cingulate, lateral

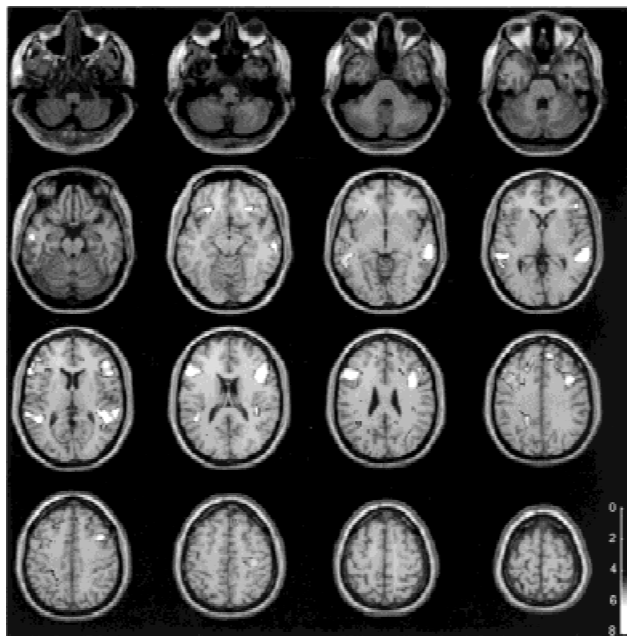


**Figure 4.** Illustration of the areas of activation for the comparison of the novel stimuli versus the target stimuli. The planes depicted are identical to those in Figure 1.

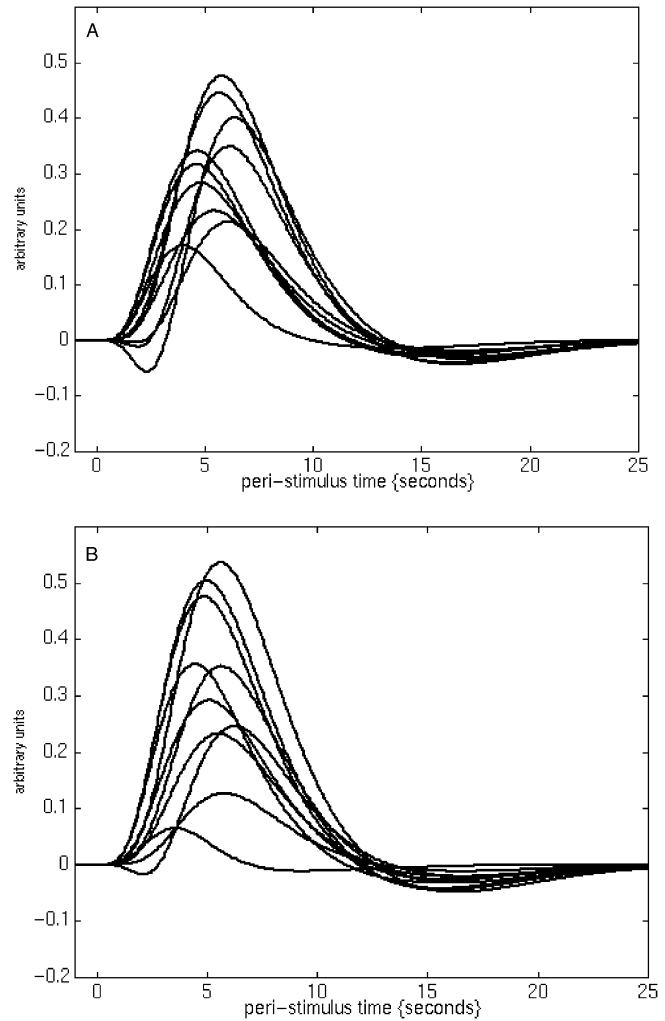


**Figure 5.** Illustration of the modeled hemodynamic response for target stimuli for each participant from a voxel located in the (A) left (Talairach coordinates:  $-41, 41, 30$ ) and (B) right (Talairach coordinates:  $34, 45, 30$ ) lateral frontal cortex.

frontal cortex, amygdala, thalamus, and putamen. There were also several modality-specific activations for auditory stimuli in primary auditory cortex and in the superior temporal gyrus that we did not observe to be activated for visual stimuli (Kiehl et al., 1999, submitted).

Analyses of the auditory novel stimuli revealed extensive bilateral temporal lobe activation. Activation also was found in the frontal lobe in the middle and inferior frontal gyrus. These data are consistent with Knight's (1984) finding that the P3a to novel stimuli is reduced in patients with prefrontal lesions. The spatial location of the middle/inferior frontal gyrus activation for novel stimuli is similar to the location observed during other tasks that involve response inhibition, but to not manipulate the novelty of the stimuli. Konishi et al. (1999) and Kiehl, Liddle, and Hopfinger (2000), using erfMRI techniques similar to those used in the present study, observed that response inhibition trials during a go/nogo paradigms activated bilateral prefrontal cortex. These data suggest that the inferior/middle frontal activation observed in the present study may be due, at least in part, to response inhibition processes placed on the subject to withhold the motor response to the novel stimuli.

**Table 4.** Summary of the Significant Areas of Activation for the Comparison of the Novel Versus Target Stimuli

Region	Talairach coordinates			z score
	x	y	z	
Frontal lobes				
1. R superior frontal gyrus	11	49	35	6.42
2. L middle frontal gyrus	-30	19	50	5.15
3. L middle/inferior frontal gyrus	-49	19	25	7.43
4. R middle/inferior frontal gyrus	42	26	25	7.25
5. L inferior frontal gyrus	-38	34	10	6.76
6. L inferior frontal gyrus/insula	-45	34	-10	5.57
7. R inferior frontal gyrus /insula	50	36	0	6.57
8. L anterior cingulate gyrus	-18	4	30	5.03
9. R anterior cingulate gyrus	22	26	30	5.41
10. R anterior cingulate gyrus	16	38	10	5.08
11. Corpus callosum	0	6	20	5.23
12. L precentral gyrus	-34	-4	40	6.01
13. R precentral gyrus	38	10	40	6.69
Parietal lobes				
14. R postcentral gyrus	38	-26	55	6.13
15. L inferior parietal lobule	-44	-34	25	5.96
16. R inferior parietal lobule	44	-34	25	5.86
17. L posterior cingulate gyrus	-19	-41	35	6.53
18. L posterior cingulate gyrus	-22	-50	10	5.55
19. L precuneus	-15	-40	40	5.73
Temporal lobes				
20. L superior/middle temporal gyrus	-49	-22	-5	5.89
21. R superior/middle temporal gyrus	64	-34	5	8.09
22. R superior/middle temporal gyrus	48	18	-20	6.47
23. R middle/inferior temporal gyrus	66	-28	-15	6.95
24. L inferior temporal gyrus	-56	0	-35	5.16
Occipital lobes				
25. L superior/middle occipital gyrus	-38	-87	25	5.95
Deep gray				
26. R putamen	34	-4	15	4.92
Cerebellum				
27. L cerebellum	-18	-50	-5	4.90

Note: L = left; R = right.

Probability levels associated with the z scores are the same as those listed in the caption to Table 1.

The observed patterns of activation for both target and novel stimuli confirm numerous studies on the intracranial distribution of neural sources activated during similar tasks. Intracranial studies have shown that target processing of auditory stimuli is associated with neural activity in the dorsolateral prefrontal cortex (e.g., middle/superior frontal gyrus), ventrolateral prefrontal cortex (e.g., inferior frontal gyrus), supramarginal gyrus (e.g., inferior parietal lobule), superior temporal sulcus, anterior and posterior cingulate, and medial temporal regions (see Halgren et al., 1998). In this study, we have confirmed that all of these regions are activated for auditory target processing using erfMRI techniques. We also observed activation for target processing in a number of other areas, including the anterior superior temporal gyrus, insula, inferior parietal lobule, and sites in the anterior frontal lobe. These latter areas not typically recorded from in intracranial studies.

Based on data from intracranial recordings, Halgren and colleagues (1998) suggested that processing rare stimuli (e.g., target and novel stimuli from the present study) is associated with activation of an orienting response. They argued that the orienting response is generated in a spatially distributed neural network, including regions of the inferior parietal lobe, cingulate, and dorsolateral prefrontal cortex. Similarly, we observed that both target and novel stimuli activated bilateral inferior parietal lobule and

dorsolateral prefrontal cortex. We also confirmed that the cingulate is activated for target processing, but we did not observe strong activation in the medial cingulate for processing novel stimuli. Halgren and colleagues also observed that the P3b response specific to target processing is associated with neural activity in the hippocampal formation, superior temporal gyrus, lateral orbital frontal gyrus, and supramarginal gyrus. Our data support this observation as well. In addition, in the direct comparison of the hemodynamic response for the target stimuli versus the novel stimuli, a comparison in ERP studies that yields a larger P3b, we observed greater activation for target than novel stimuli bilaterally in the middle frontal gyrus, anterior superior temporal gyrus, hippocampal formation, insula, thalamus, superior temporal gyrus, and superior and inferior parietal lobule (e.g., supramarginal gyrus). Thus, we have confirmed and extended the results of intracranial studies of target detection and novelty processing.

In the present study, we were interested in examining the role of all the neural systems involved with target detection, including the motor system. However, it is important to note that during this task we required a manual response to target stimuli that raises the issue that some areas of activation we observed for target processing may be related to the motor response and not to target processing per se. The results from a recently completed study from

our laboratory in which we had participants silently count the target stimuli, rather than respond to them, helps address which neural areas might be involved in the motor response (Kiehl et al., submitted). In that study, we observed that the same areas of activation for both target and novel stimuli as we did in the present study, with the exception of motor cortex and cerebellum. Thus, we are confident that the areas of activation outside these two regions are more likely related to target detection than to some aspects of motor processing.

The present study used a relatively small sample size, which raises the possibility that some of the results are sample specific. However, in two subsequent studies from our laboratory we have observed complete replication of the present results for both target and novel stimuli (Kiehl & Liddle, 1999b). We have also shown that the areas of activation observed for target processing are reproducible in the same subjects after 6 weeks in a test-retest study (Kiehl & Liddle, 1999b). Nevertheless, despite the apparent reliability of these effects, we must note that the erfMRI analysis techniques used in the present study remain controversial (e.g., McCarthy et al., 1997).

Although the implication of the present results for localizing generators of the ERP elicited during similar tasks is still uncertain, some tentative conclusions can be drawn. ERP oddball tasks have shown that target processing elicits a complex component structure, the most prominent of which are an N2, P3, and a slow wave. In large part, source-modeling studies have shown that the N2 component is localized to the temporal lobe, specifically the superior/middle temporal gyrus. In the present study, we observed activation in these regions for both target and novel stimuli. Further support for this localization of the N2 component comes from a recently completed study in our laboratory in which we had subjects detect "gaps" in an otherwise continuous stream of auditory stimuli (Kiehl & Liddle, 1999a). ERP studies using similar tasks have shown that the N2 response to these stimuli is absent, yet a strong P3 and slow wave remains (Friedman, 1984; Sutton et al., 1967). In the present study, we replicated all the areas of activation for target stimuli observed in the present study except that aspects of the middle/superior temporal gyrus were not observed to be activated. Thus, on balance, these data suggest that the N2 component is related to neural activity emanating from bilateral superior/middle temporal gyrus.

The relationship between the areas of activation observed in the present study and the localization of the sources of the P3 and slow wave are, however, more complex. Indeed, we note that it is also plausible that some of the areas of activation observed in the present study may be specific to hemodynamic imaging (e.g., slow affective processing). Nevertheless, in the present study we have replicated the results of many intracranial studies of the oddball processing (e.g., Halgren et al., 1998), which are considered the "gold" standard of source localization. In large part, these intracranial studies, and the data from the present study, support the notion that target processing and novelty detection are associated with activation of multiple, spatially distributed parallel processing systems. Indeed, Halgren and colleagues have suggested that the brain seems to adopt the strategy of engaging all potentially useful areas, even though the probability may be very low that they will contribute to immediate task performance. Such a strategy, although not necessary for simple psychological tasks, may have been advantageous, in an evolutionary sense. The ability to rapidly identify, evaluate, and coordinate neural activity to execute a behavioral response and/or withhold a behavioral response would lead to a longer survival and better reproductive rates (see Halgren et al., 1998, for more). Thus, these data provide strong support for the hypothesis that the brain utilizes multiple parallel processing pathways during even simple cognitive tasks (see also Aguirre, Zarahn, & D'Esposito, 1998; Mesulam, 1990, 1994; Morecraft, Geula, & Mesulam, 1993).

In conclusion, we have observed that target detection and novelty processing in both the auditory and visual modalities activate a concert of spatially remote cortical areas. The spatial locations that we have observed to be activated by target detection and novelty processing are consistent with the intracranial distribution of the neural sources generated during similar tasks. However, using erfMRI, we were able to examine the entire brain, which revealed numerous additional areas of activation associated with target detection and novelty processing not previously observed to be involved in these tasks. Finally, these data support the hypothesis that processing of even simple cognitive tasks is associated with a widespread activation of multiple parallel systems that engage potentially all relevant brain areas to rapidly evaluate and process stimuli.

## REFERENCES

- Aguirre, G. K., Zarahn, E., & D'Esposito, M. (1998). The inferential impact of global signal covariates in functional neuroimaging analyses. *Neuroimage*, *8*, 302-306.
- Alexander, J. E., Bauer, L. O., Kuperman, S., Morzorati, S., O'Connor, S. J., Rohrbaugh, J., Porjesz, B., Begleiter, H., & Polich, J. (1996). Hemispheric differences for P300 amplitude from an auditory oddball task. *International Journal of Psychophysiology*, *21*, 189-196.
- Andersson, J. L. (1997). How to estimate global activity independent of changes in local activity. *Neuroimage*, *6*, 237-244.
- Boynton, G., Engel, S., Glover, G., & Heeger, B. (1996). Linear systems analysis of functional magnetic resonance imaging in human V1. *Journal of Neuroscience*, *16*, 4207-4221.
- Buckner, R. L. (1998). Event-related fMRI and the hemodynamic response. *Human Brain Mapping*, *6*, 373-377.
- Dale, A. M., & Buckner, R. (1997). Selective averaging of rapidly presented individual trials using fMRI. *Human Brain Mapping*, *5*, 329-340.
- D'Esposito, M., Zarahn, E., & Aguirre, G. K. (1999). Event-related functional MRI: Implications for cognitive psychology. *Psychological Bulletin*, *125*, 155-164.
- Donchin, E., & Coles, M. G. H. (1988). Is the P300 component a manifestation of context updating? *Behavior and Brain Sciences*, *11*, 357-374.
- Ford, J. M., White, P. M., Csernansky, J. G., Faustman, W. O., Roth, W. T., & Pfefferbaum, A. (1994). ERPs in schizophrenia: Effects of antipsychotic medication. *Biological Psychiatry*, *36*, 153-170.
- Fox, P. T., Mintun, M. A., Reiman, E. M., & Raichle, M. E. (1988). Enhanced detection of focal brain responses using intersubjects and change distribution analyses of subtracted PET images. *Journal of Cerebral Blood Flow and Metabolism*, *8*, 642-653.
- Friedman, D. (1984). Cognitive brain potential components in adolescents. *Psychophysiology*, *21*, 83-96.
- Friston, K. J., Ashburner, J., Frith, C. D., Poline, J. -B., Heather, J. D., & Frackowiak, R. S. J. (1995a). Spatial registration and normalization of images. *Human Brain Mapping*, *2*, 165-189.
- Friston, K. J., Fletcher, P., Josephs, O., Holmes, A., Rugg, M. D., & Turner, R. (1998). Event related fMRI: Characterizing differential responses. *NeuroImage*, *7*, 30-40.
- Friston, K. J., Frith, C. D., Liddle, P. F., Dolan, R. J., Lammertsma, A. A., & Frackowiak, R. S. (1990). The relationship between global and local changes in PET scans. *Journal of Cerebral Blood Flow and Metabolism*, *10*, 458-466.
- Friston, K. J., Holmes, A. P., Worsley, K. J., Poline, J. -P., Frith, C. D., & Frackowiak, R. S. J. (1995b). Statistical parametric maps in func-

- tional imaging: A general linear approach. *Human Brain Mapping*, 2, 189–210.
- Friston, K. J., Jezzard, P., & Turner, R. (1994). Analysis of functional MRI time series. *Human Brain Mapping*, 1, 153–171.
- Friston, K. J., Williams, S., Howard, R., Frackowiak, R. S. J., & Turner, R. (1996). Movement-related effects in fMRI time-series. *Magnetic Resonance in Medicine*, 35, 346–355.
- Friston, K. J., Zarahn, E., Josephs, O., Henson, R. N. A., & Dale, A. M. (1999). Stochastic designs in event-related fMRI. *NeuroImage*, 10, 607–619.
- Halgren, E., Marinkovic, K., & Chauvel, P. (1998). Generators of the late cognitive potentials in auditory and visual oddball tasks. *Electroencephalography and Clinical Neurophysiology*, 106, 156–164.
- Holmes, A. P., Josephs, O., Buchel, C., & Friston, K.J. (in press). Statistical modelling of low frequency confounds in fMRI. *Human Brain Mapping*.
- Josephs, O., Turner, R., & Friston, K. (1997). Event-related fMRI. *Human Brain Mapping*, 5, 1–7.
- Kiehl, K. A., Hare, R. D., McDonald, J. J., & Liddle, P. F. (1999). Reduced P3 responses in criminal psychopaths during a visual oddball task. *Biological Psychiatry*, 45, 1498–1507.
- Kiehl, K. A., Laurens, K. R., Duty, T. L., Forster, B. B., & Liddle, P. F. (1999). *An event-related fMRI study of a visual oddball task*. Manuscript submitted for publication.
- Kiehl, K.A., Laurens, K.R., Desjardins, A.E., & Liddle P.F. (1999). The effect of task demands on the hemodynamic response to auditory oddball stimuli: An event-related fMRI study. Manuscript submitted for publication.
- Kiehl, K.A., & Liddle, P.F. (in press). An event-related fMRI study of an auditory oddball task in schizophrenia. *Schizophrenia Research*.
- Kiehl, K. A., & Liddle, P. F. (1999a). *The missing stimulus: An event-related fMRI study*. Manuscript in preparation.
- Kiehl, K. A., & Liddle, P. F. (1999b). *Reproducibility of the hemodynamic response to auditory oddball stimuli: A test-retest study*. Manuscript in preparation.
- Kiehl, K. A., Liddle, P. F., & Hopfinger, J. B. (2000). Error processing and the rostral anterior cingulate: An event-related fMRI study. *Psychophysiology*, 37, 216–223.
- Knight, R. T. (1984). Decreased response to novel stimuli after prefrontal lesions in man. *Electroencephalography and Clinical Neurophysiology: Evoked Potentials*, 59, 9–20.
- Konishi, S., Nakajima, K., Uchida, I., Kikyo, H., Kameyama, M., & Miyashita, Y. (1999). Common inhibitory mechanism in human inferior prefrontal cortex revealed by event-related functional MRI. *Brain*, 122, 981–991.
- McCarley, R. W., Faux, S. F., Shenton, M. E., Nestor, P. G., & Adams, J. (1991). Event-related potentials in schizophrenia: Their biological and clinical correlates and a new model of schizophrenic pathophysiology. *Schizophrenia Research*, 4, 209–231.
- McCarthy, G., Luby, M., Gore, J., & Goldman-Rakic, P. (1997). Infrequent events transiently activate human prefrontal and parietal cortex as measured by functional MRI. *Journal of Neurophysiology*, 77, 1630–1634.
- Menon, V., Ford, J. M., Lim, K. O., Glover, G. H., & Pfefferbaum, A. (1997). Combined event-related fMRI and EEG evidence for temporal-parietal cortex activation during target detection. *NeuroReport*, 8, 3029–3037.
- Mesulam, M. M. (1990). Large-scale neurocognitive networks and distributed processing for attention, language, and memory. *Annals of Neurology*, 28, 597–613.
- Mesulam, M. M. (1994). Neurocognitive networks and selectively distributed processing. *Revue Neurologique*, 150, 564–569.
- Morecraft, R. J., Geula, C., & Mesulam, M. M. (1993). Architecture of connectivity within a cingulo-fronto-parietal neurocognitive network for directed attention. *Archives of Neurology*, 50, 279–284.
- Opitz, B., Mecklinger, A., Von Cramon, D. Y., & Kruggel, F. (1999). Combining electrophysiological and hemodynamic measures of the auditory oddball. *Psychophysiology*, 36, 142–147.
- Rosen, B. R., Buckner, R. L., & Dale, A. M. (1998). Event-related functional MRI: Past, present, and future. *Proceedings of the National Academy of Sciences of the United States of America*, 95, 773–780.
- Sutton, S., Tueting, P., Zubin, J., & John, E. R. (1967). Information delivery and the sensory evoked potential. *Science*, 155, 1436–1439.
- Worsley, K. J. (1994). Local maxima and the expected Euler characteristic of excursion sets of  $\chi^2$ ,  $F$  and  $t$  fields. *Advances in Applied Probability*, 26, 13–42.
- Worsley, K. J., & Friston K. J. (1995). Analysis of fMRI time-series revisited—Again. *Neuroimage*, 2, 173–181.

(RECEIVED October 26, 1998; ACCEPTED February 24, 2000)